International Journal of Marine Engineering Innovation and Research, Vol. 8(2), Jun. 2023. 222-231
(pISSN: 2541-5972, eISSN: 2548-1479)

Leading Edge Modification of NACA 0015 and NACA 4415 Inspired by Beluga Whale

James Julian[1], Waridho Iskandar[2], Fitri Wahyuni[3]
(Received: 24 March 2023 / Revised: 20 April 2023 /Accepted: 03 May 2023)

***Abstract*— This research modifies the leading-edge structure of NACA 0015 and NACA 4415 to resemble the nose of a beluga whale. The focus of this modification is to improve the airfoil's aerodynamic performance and investigate the changing fluid flow patterns. Numerical equation used is RANS combined with the *k-ε* turbulence model. Mesh independence test shows that mesh with 200 elements is the best mesh. Validation results reveal that CFD data can follow the trend of experimental data, especially on the AoA before the stall. There was a significant increase in C_l from NACA 0015 and NACA 4415 at AoA>9°. On the other hand, the modification also had a positive effect by lowering the C_d value. The modification also provides an advantage by increasing the maximum C_l/C_d value. Furthermore, the separation point data shows that the modification can delay the separation of the fluid flow in the airfoil. Modifications can cause an increase in pressure on the lower side and a decrease in pressure on the upper side. Through velocity contours and streamlines, the modifications can reduce the recirculation area. Overall, modifying the leading edge has positive impacts on the NACA 0015 and NACA 4415 airfoils.**

Keywords—beluga whale, efficiency, Modification, NACA 0015, NACA 4415

I. INTRODUCTION

Increasing the aerodynamic efficiency of the airfoil is an interesting problem to be studied further. An airfoil can be considered efficient if it can produce a high lift force while keeping the drag force as low as possible [1] [2]. If the airfoil's shape is applied to the plane, the airfoil with a high lift force will make it easier for the plane to take off. Meanwhile, if the airfoil can reduce the drag force, it will help the plane save fuel during the flight[3][4]. Airfoil efficiency becomes more vital when the airfoil is applied to the glider. The glider is an aircraft that can work efficiently and does not require a propulsion system to fly and stay in the air for a long time [5]. In wind turbines, the lift force generated by the interaction between the turbine blades and the wind blow is used to rotate the turbine blades [6] [7]. There are various ways to increase the lift force of the airfoil, one of which is by increasing the fluid velocity. Flow control devices can increase the efficiency of airfoil. Several flow control devices can help increase airfoil efficiency by increasing lift, reducing drag and even both [8] [9]. Another way to be used is modifying the baseline shape of the airfoil. Modifying the baseline shape of the airfoil in this study was done by changing the shape of the airfoil's leading edge to resemble the nose of a beluga whale.

Arabaci and Pakdemirli had adapted the nose of the beluga whale on the bus. The research was conducted to reduce the drag force on the bus on the stationary road and move road conditions. The analysis was carried out at an inlet velocity of 16.66 m/s. It concludes that the optimum shape of the beluga nose can reduce the bus's C_d by 27.4% in stationary road conditions. In moving road conditions, the optimum shape of the nose of the beluga whale can reduce C_d by 20.17% [10]. Chowdhury et al., 2018 modified the front surface of a passenger car by adapting the boxfish's shape. The analysis was performed using the CFD method. The CFD process is carried out at various speeds ranging from 40 km/h to 100 km/h. Modifying the boxfish shape can reduce the drag coefficient from the original 0.56 to 0.28 at all speed variations [11]. Another research has been done by adapting the crescent tails in Thunnus thynnus, sailfish, isurus oxyrhynchus and swordfish. The aim is to reduce the vortex behind ahmed body so that it can reduce C_d. The shape of the crescent-type tails is modeled by installing an elliptical flap on the back of the body. The angle between the elliptical flap and the vertical line that produces the best performance is 50º. The use of an elliptical flap can reduce C_d up to 11.1% [12]. Peng et al., 2017 also researched reducing C_d in vehicles by applying the tiger beetle body shape. The shape of the vehicle's upper body is modified to match the curved shape of the tiger beetle. Modifications can help the car reduce C_d from 0.28 to 0.29 [13]. Sudhakar and Karthikeyan conducted an experimental study on the NACA 4415 airfoil by implementing tubercles on the leading edge. Tubercles can be found on the fins of humpback whales. Tubercles on the airfoil at a low Reynolds number can reduce separation up to 50% at AoA=18° [14].

Some of the studies mentioned above are held to improve the aerodynamic capabilities of a body shape using methods inspired by animals that exist in nature. However, many of these studies focused on vehicle modification to reduce the C_d. Therefore, those studies

James Julian, Department of Mechanical Engineering, Universitas Pembangunan Nasional Veteran Jakarta, Jakarta, 12450, Indonesia. E-mail: zames@upnvj.ac.id
Waridho Iskandar, Department of Mechanical Engineering, Universitas Pembangunan Nasional Veteran Jakarta, Jakarta, 12450, Indonesia. E-mail: waridho.iskandar@upnvj.ac.id
Fitri Wahyuni, Department of Mechanical Engineering, Universitas Pembangunan Nasional Veteran Jakarta, Jakarta, 12450, Indonesia. E-mail: fitriwahyuni@upnvj.ac.id

cannot be used as a robust parameter when discussing airfoils because airfoils can generate lift force. In addition, the airfoil also has a special feature in the form of a streamlined shape so that the resulting fluid flow conditions are very different from vehicles. Research conducted by Sudhakar and Karthikeyan also only focuses on fluid flow separation without considering essential parameters such as aerodynamic forces and the efficiency of the airfoil.

This paper analyzes and investigate the aerodynamic capabilities of the modified NACA 4415 and NACA 0015 airfoils by adapting the nose shape of the beluga whale. This study also assessed the aerodynamic performance resulting from these modifications and compared them with the baseline forms of NACA 4415 and NACA 0015. Thus, a comprehensive conclusion can be drawn about whether this modification can significantly impact the aerodynamic efficiency of the airfoil. In particular, this study also aims to see the differences in fluid flow patterns between modified and unmodified airfoils. Furthermore, this study also tries to reveal the effect of symmetrical and asymmetrical airfoils on the effectiveness of the beluga whale's nose shape

II. METHOD

A. NACA four digit

The four-digit NACA is an airfoil introduced by the National Advisory Committee for Aeronautics (NACA). The distribution thickness of the four-digit NACA has almost the same shape as some efficient airfoils, such as the Göttingen 398 and Clark Y airfoil. NACA four-digit can be created by at least 50 points or more. The advantage of the four-digit NACA is that it has good stall characteristics, has a relatively low center of pressure movement and has little effect on roughness. As the name implies, the four-digit NACA consists of four integer digits. The first integer is the maximum camber of the airfoil and the second integer indicates the maximum position of the camber. The third and fourth integers are the maximum thickness of the airfoil [15] [16]. A symmetrical four-digit NACA must have the first and second integers being zero, and this is because the airfoil has the same camber line as the chord line. The camber line is defined as a line that divides the airfoil in equal size. Meanwhile, the chord line is a line that start form leading edge to trailing edge [17]. The four-digit NACA used as objects in this study is NACA 4415 and NACA 0015, as seen in Figure 1.

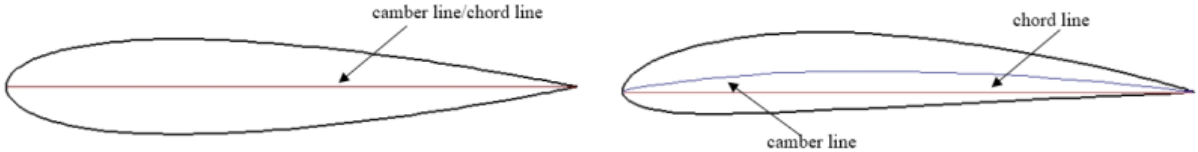

(a) NACA 0015 (b) NACA 4415

Figure 1. NACA four-digit

B. Modification of airfoils

The leading edges of the NACA 4415 and NACA 0015 were modified by applying a beluga whale nose shape. The dimensions of this modification can be seen in Figure 2. This dimension was first introduced by Mohamed et al [18]. All dimensions are shown in the form of multiplication of the values of c. The symbol c is the length of the airfoil chord [19]. In this study, the chord length of NACA 0015 and NACA 4415 is 1 meter [20]. The final form of NACA 4415 and NACA 0015 after modification can be seen in Figure 3.

C. Numerical method and turbulence model

The case of fluid flow around the airfoil in this research is solved by using a numerical method or can be known as CFD. RANS equation can regulate incompressible fluid flow [21]. RANS equation consists of the momentum equation and the mass conservation equation. Both of them are given in equation 1 and equation 2, respectively [22]. RANS equation can be completed by using the $k-\varepsilon$ turbulence model is used. The $k-\varepsilon$ equation has its advantages in predicting the coefficients of aerodynamic forces [23]. The equations for the $k-\varepsilon$ turbulence model are written in equations 3 and 4 [24].

$$\frac{\partial \rho}{\partial t}+\frac{\partial}{\partial x_i}(\rho u_i)=0 \tag{1}$$

$$\frac{\partial}{\partial t}(\rho u_i)+\frac{\partial}{\partial x_i}(\rho u_i u_j)= \frac{\partial p}{\partial x_i}+\frac{\partial}{\partial x_j}\left[\mu\left(\frac{\partial u_i}{\partial x_j}+\frac{\partial u_j}{\partial x_i}-\frac{2}{3}\delta_{ij}\frac{\partial u_i}{\partial x_i}\right)\right] +\frac{\partial}{\partial x_i}\left(-\rho\overline{u_i' u_j'}\right) \tag{2}$$

$$\frac{D}{Dt}(\rho k)=\frac{\partial}{\partial x_j}\left[\left(\mu+\frac{\mu_t}{\sigma_k}\right)\frac{\partial k}{\partial x_j}\right]+G_k-\rho\varepsilon \tag{3}$$

$$\frac{D}{Dt}(\rho \varepsilon)=\frac{\partial}{\partial x_j}\left[\left(\mu+\frac{\mu_t}{\sigma_\varepsilon}\right)\frac{\partial \varepsilon}{\partial x_j}\right]+C_{e1}\frac{\varepsilon}{k}G_k -\rho C_{\varepsilon 2}\frac{\varepsilon^2}{k} \tag{4}$$

D. Mesh, domain and setup conditions

This research uses structured mesh. The mesh uses a quadrilateral shape, as seen in Figure 4(a). The mesh

Figure 2. Dimension of modification

is made denser as it approaches the airfoil [25]. Meanwhile, the shape of the domain and its dimensions are illustrated in Figure 4(b). Details of the boundary conditions can be found in Figure 4(c). Boundary conditions in the domain consist of velocity-inlet and pressure-outlet. Meanwhile airfoil defined as wall (no-slip) boundary conditions [26].

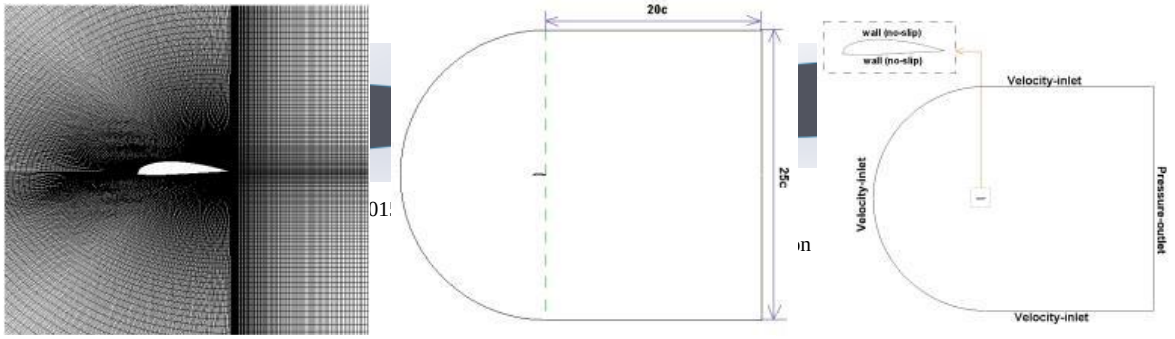

(a) Mesh (b) Domain (c) Bounday condition

Figure. 4. Pre-processing parameters

E. Mesh independence test

The mesh independence test in this study used the method proposed by Roache. Various equations are needed to perform the mesh independence test. Equation 5 describes the ratio of the number of mesh elements. The order of the mesh independence test is written in equation 6. Meanwhile, the grid convergence index for the fine mesh can be determined using equation 7[27]. Besides, the grid convergence index for the coarse mesh is determined by equation 8. Error band can be calculated by equations 9 and 10[28]. The Mesh independence test is carried out by testing three mesh variations, i.e., fine (200000 elements), medium (100000 elements) and coarse (50000 elements), as shown in Figure 5. The purpose of this step is to find out the mesh with the lowest error and ensure that the results given by each mesh variation are in the convergence index range. The mesh independence test takes samples of fluid velocity values around NACA 0015 at x=0.5 and y=0.5 with AoA=0º. The sample is expressed as a discrete solution (f). The results are given in table 1. Variation of the mesh in this study can be said in the convergence index range after the $\frac{GCI_{coarse}}{GCI_{fine}r^{\bar{p}}} \approx 1.0007$ [29]. The GCI_{fine} is equal to 0.019% and the GCIcoarse is 0.1185%. Mesh selected for further computation is fine because it has the smallest error value, i.e., 0.0154%. Mesh error is the error between a discrete solution and the exact value. Equation 12 can be used to calculate the exact value.

$$r = \frac{h_{fine}}{h_{medium}} = \frac{h_{medium}}{h_{coarse}} \tag{5}$$

$$\bar{p} = \frac{\ln\left(\frac{f_{fine} - f_{medium}}{f_{medium} - f_{coarse}}\right)}{\ln(r)} \tag{6}$$

$$GCI_{fine} = \frac{F_s \,|\epsilon_{fine}|}{\left(r^{\bar{p}} - 1\right)} \tag{7}$$

$$GCI_{coarse} = \frac{F_s \,|\epsilon_{coarse}|\, r^{\bar{p}}}{\left(r^{\bar{p}} - 1\right)} \tag{8}$$

$$\epsilon_{fine} = \frac{f_{fine} - f_{medium}}{f_{medium}} \tag{9}$$

$$\epsilon_{coarse} = \frac{f_{medium} - f_{coarse}}{f_{coarse}} \tag{10}$$

$$\frac{GCI_{coarse}}{GCI_{fine}r^{\bar{p}}} \approx 1 \tag{11}$$

$$f\,r_{h=0} = f_{fine} + \frac{(f_{fine} - f_{medium})}{\left(r^{\bar{p}} - 1\right)} \tag{12}$$

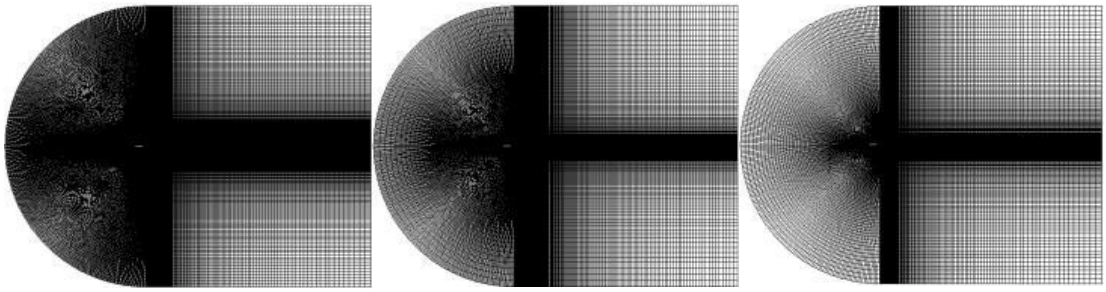

(a) Fine (b) Medium (c) Coarse

Figure. 5. Mesh in this study

TABLE 1.
RESULTS OF MESH STUDY

Type	Variable(u)	$\bar{p}$	r	$f_{h=0}$	Mesh error
fine	15.2841				0.0154%
medium	15.2719	2.6204	2	15.2864	0.0947%
coarse	15.1974				0.5822%

III. Results and Discussion

The comparison between experimental results and CFD is shown in Figure 6. This comparison is a validation to ensure that the data obtained from computational can be well received. C_l and C_d data on the baseline airfoil NACA 0015 and NACA 4415 are the main data in this validation stage. These two airfoils were analyzed at different Reynolds numbers following the experimental data that have been available from other studies. The computational process for NACA 0015 is performed on the Reynolds number 160000 [30]. Meanwhile, the computational process for NACA 4415 is performed on the Reynolds number 3000000 [31]. Based on Figure 6(a), it can be observed that the experimental data and computational data on NACA 0015 show similar results where the C_l curve is a drop curve [32]. Stalls from experimental and computational data also occur in the same AoA. Sufficiently identical results can also be observed in the C_l data for the NACA 4415 airfoil. However, the stall is delayed one degree compared to experimental data. Figure 6(b) is the C_d data from computational and experimental results on NACA 4415 and NACA 0015. All C_d data on AoA≤10º show almost similar results in all types of airfoils. When AoA>10º, NACA 0015 data started to show quite different results. NACA 4415 showed different results between computational and experimental data when AoA>15º. Overall, the C_l and C_d data showed quite valid results, especially in AoA before the stall. After the stall, the C_l and C_d data begin to show deviations. This deviation is acceptable because of the weakness of the RANS equation in modeling fluid flow conditions in post-stall conditions. In addition, a complex vortex has been formed when the airfoil is in a post-stall condition, so the fluid flow condition has become unstable [33].

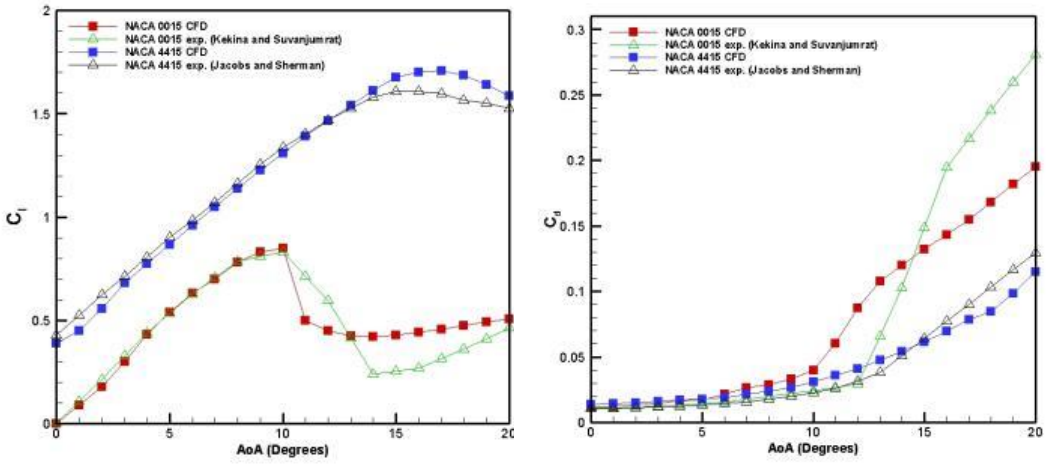

(a) C_l (b) C_d

Figure. 6. Validation

The C_l data for NACA 0015 and NACA 4415 before and after modification can be seen in Figure 7(a). The Reynolds number used in this data is 10^6, which applies to all types of airfoils and their modifications. At AoA≤4º, airfoil modification did not significantly affect changes in C_l values in NACA 0015 and NACA 4415. The increase in C_l in airfoils slowly began to be seen

when AoA>4º. However, the modification to NACA 0015 cannot delay the stall where it stalls but occurs at AoA=14º. Different results are seen on the NACA 4415 where the airfoil can delay the stall even though it is only one degree. Baseline NACA 4415 occurred stall at AoA=14º. Meanwhile, the stall after modification is at AoA=15º. Figure 7(b) is the C_d data on NACA 0015 and NACA 4415 before and after modification. The leading-edge modification of airfoils has a positive effect by lowering the C_d value. The decrease in the value of C_d in NACA 0015 begins at AoA≥3º, and the decrease in NACA 4415 begins at AoA≥4º.

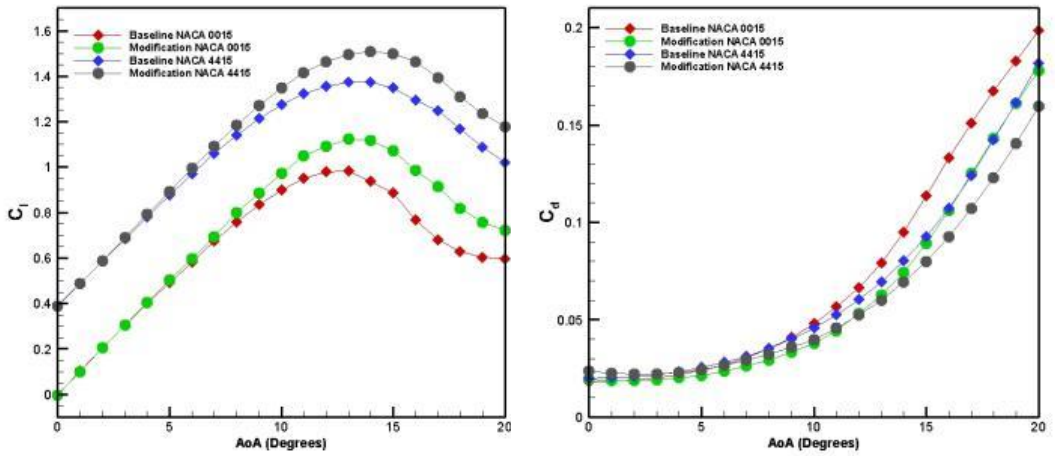

(a) Lift coefficient of airfoil

(b) Drag coefficient of airfoil

Figure. 7. Aerodynamic data

The efficiency of NACA 0015 and NACA 4415 before and after modification can be seen in Figure. 8. Modifying NACA 0015 at 0º≤AoA≤3º cannot increase the airfoil efficiency due to the increase in the C_d value. A very satisfactory result is seen at AoA>3º, where airfoils that have been modified can improve the efficiency very well. Baseline NACA 0015 has maximum efficiency at AoA=7º. Meanwhile, the maximum efficiency after NACA 0015 has been modified is at AoA=8º. The modified NACA 4415 occur a decrease in performance at AoA<3º. After that, modified NACA 4415 showed satisfactory results. Baseline NACA 4415 has the highest efficiency at AoA=6º, and the modified NACA 4415 has the highest maximum efficiency at AoA=7º. Thus, it can be concluded that the modification of the airfoil can increase the maximum efficiency of the airfoil and can increase the AoA with a maximum efficiency of one degree.

This analysis was carried out to investigate whether modification of the airfoil's shape can delay or even eliminate separation. This analysis is also helpful for knowing how the airfoil improves its efficiency or aerodynamic performance. The location of the separation is a parameter commonly used to measure the reliability of a fluid flow control device [34] [35]. A fluid flow control device can be declared reliable if it can delay or even eliminate separation [36], [37]. Separation is a phenomenon that is highly avoided in airfoils [38]. Separation is a major cause of stalled airfoils [39]. The location of the separation points at NACA 0015 and NACA 4415 is given in Figure 9. The separation points are written in the form of a dimensionless value. This dimensionless value is

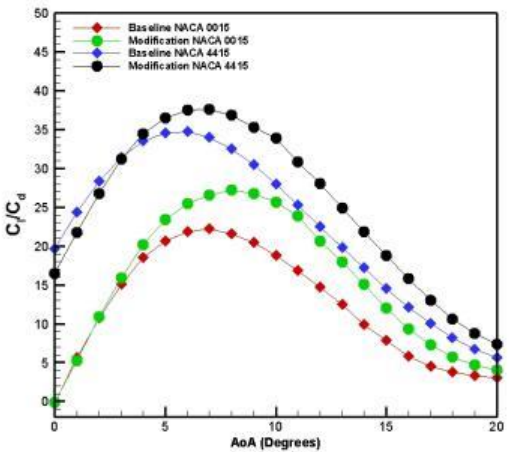

Figure 8. Efficiency of airfoils with and without modification

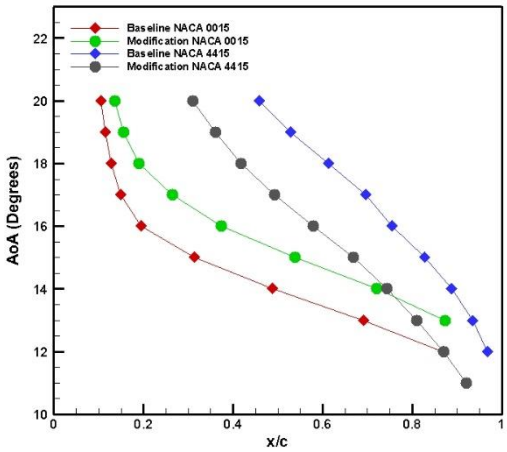

Figure 9. Fluid flow separation position

obtained from the ratio between the separation point location and the chord length. The purpose of using this ratio is that the results obtained can be generalized regardless of the chord length of the airfoil. Modification of NACA 0015 can delay the occurrence of separation. Separation at baseline NACA 0015 begins to occur at AoA=12º. Meanwhile, separation in modification NACA 0015 begins at AoA=13º. Modifying NACA 0015 can also shift the separation closer to the trailing edge [40]. This applies to all AoAs. At the extreme AoA, the shift in the location of the separation is not very significant. A contrasting result is seen in NACA 4415. Modification of the NACA 4415 can shift the separation location in the near of leading edge. In addition, the modification also precedes the separation. At baseline NACA 4415, separation begin AoA=12º. However, in the modified NACA 4415 the separation begins at AoA=11º. It is necessary to investigate further whether the phenomenon of accelerating separation occurs only in the modified NACA 4415 or in all four-digit NACA asymmetry.

The fluid flow around the airfoil is visualized through the pressure contour, as shown in Figure 10. At AoA=0º, the modification of airfoils does not give the effect on the pressure of fluid around the airfoil. The modification airfoil shifts the area with the highest pressure to the beginning of the upper side. The high pressure is converted to pressure C_d so that the C_d received by the airfoil is greater than the baseline airfoil. In addition, this increase in pressure also slightly decreases the C_l ability of the airfoil. Thus, the modified airfoil is not very suitable for use at low AoA. When AoA=10º, the modified NACA 0015 and the baseline NACA 0015 have nearly identical pressure contours.

The increase in C_l in the modified NACA 0015 is caused by the increase in the area in direct contact with the high-pressure fluid, namely in the modified area.On the other hand, the pressure on the upper side tends not to increase so that the C_l can increase properly. On the NACA 4415, the increase in pressure near bottom side is visible. However, the increase in pressure on the top side also occurs, so the increase in C_l produced by NACA 4415 is not as good as NACA 0015. Velocity contours and fluid flow streamlines are used to visualize the fluid flow separation on the airfoil's upper side. Two AoA, i.e., AoA=15º and AoA=20º, are used as samples in this analysis. Overall, the velocity and streamline contours of the fluid flow in this paper are given in Figure 11. Based on Figures 11 (a) and 11 (b), the modification of NACA 0015 not only shifts the separation location towards the leading edge but also reduces the fluid flow separation area. Contrasting results are seen in the case of flow around NACA 4415. In NACA 4415, the modification causes the fluid flow separation to expand. That is why the increase in performance of NACA 4415 is not as good as NACA 0015. Therefore, the performance improvement of NACA 4415 is entirely caused by pressure differences on the upper and lower sides. The same pattern is also seen at AoA=20º. Because the fluid flow separation initially occurs at the trailing edge and then expands to the leading edge, the stall can be said to be a trailing edge stall type.

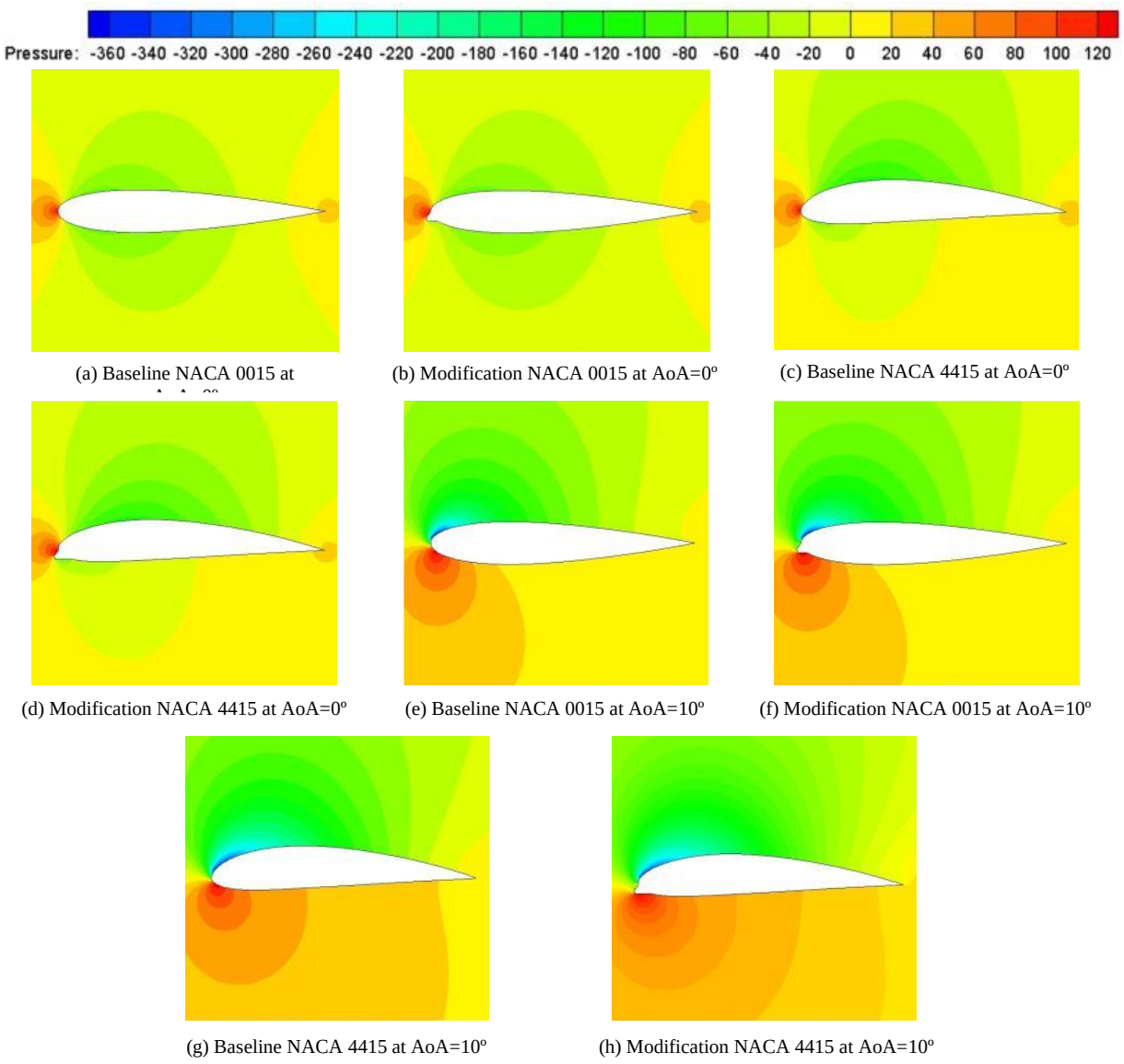

(a) Baseline NACA 0015 at

(b) Modification NACA 0015 at AoA=0º

(c) Baseline NACA 4415 at AoA=0º

(d) Modification NACA 4415 at AoA=0º

(e) Baseline NACA 0015 at AoA=10º

(f) Modification NACA 0015 at AoA=10º

(g) Baseline NACA 4415 at AoA=10º

(h) Modification NACA 4415 at AoA=10º

Figure. 10. Pressure contour

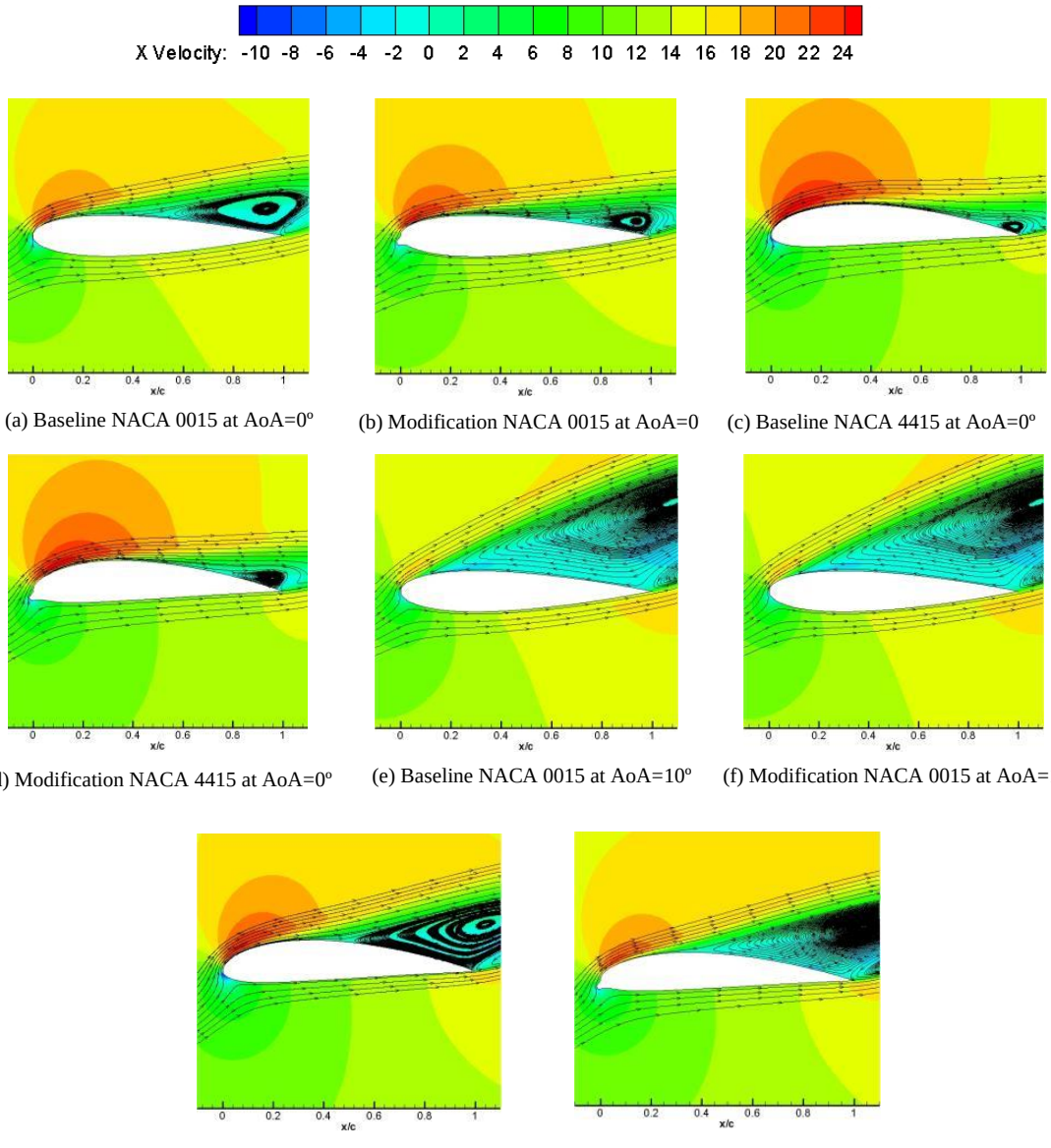

(a) Baseline NACA 0015 at AoA=0º (b) Modification NACA 0015 at AoA=0 (c) Baseline NACA 4415 at AoA=0º

(d) Modification NACA 4415 at AoA=0º (e) Baseline NACA 0015 at AoA=10º (f) Modification NACA 0015 at AoA=10º

(g) Baseline NACA 4415 at AoA=10º (h) Modification NACA 4415 at AoA=10º

Figure. 11. Velocity contour

IV. CONCLUSION

Modification is conducted on NACA 0015 and NACA 4415 by adapting the shape of the beluga whale's nose. The result obtained is that the modified airfoil can increase the value of C_l and reduce C_d. Modifying NACA 0015 and NACA 4415 can increase the efficiency of the airfoil, mainly at AoA≥3º. Thus, it can be concluded that the modification of the airfoil positively impacts the aerodynamic efficiency. The fluid flow when AoA=0º around the modified airfoil tends to change slightly in the form of a shift in the high-pressure area towards the upper side. So that at AoA=0º, the airfoil experienced a slight decrease in C_l and an increase in C_d. If AoA°, the pressure on bottom of modified NACA 0015 is slightly increase. When AoA=10º, the modification of NACA 0015 slightly increased the pressure on the bottom area. The pressure on the top side tends to be constant, so the additional C_l produced is quite large. Meanwhile, at NACA 4415, there is a pressure increase on the bottom of airfoil. However, the pressure on top of airfoil also increased, so the percentage increase in C_l was not as good as NACA 0015. Overall, the efficiency improvement of NACA 0015 after modification was indeed better than NACA 4415 after modification. However, this efficiency increase cannot even match the baseline efficiency of NACA 4415. However, NACA 0015 provides better results from the point of view of separation. NACA 0015 can delay separation and shift the separation point closer to the leading edge. It is in stark contrast to the modification of NACA 4415, which precede separation and shifts separation closer to the leading edge.

This study provides an initial description of the modification of the leading edges airfoil that applies the shape of the nose of the beluga whale. Further research is needed to develop this research. Various variations of symmetrical and asymmetrical airfoils also need to be considered for further research to conform to everything revealed. The modified airfoil can also be analyzed in 3 dimensions to get more actual data. In addition, the AoA variation can also be enlarged in order to obtain comprehensive information.

REFERENCES

[1] S. E. James, A. Suryan, J. J. Sebastian, A. Mohan, and H. D. Kim, "Comparative study of boundary layer control around an ordinary airfoil and a high lift airfoil with secondary blowing," *Comput Fluids*, vol. 164, pp. 50–63, 2018, doi: https://doi.org/10.1016/j.compfluid.2017.03.012.

[2] Harinaldi, M. D. Kesuma, R. Irwansyah, J. Julian, and A. Satyadharma, "Flow control with multi-DBD plasma actuator on a delta wing," *Evergreen*, vol. 7, no. 4, pp. 602–608, 2020, doi: 10.5109/4150513.

[3] Z. Mohamed-Kassim and A. Filippone, "Fuel savings on a heavy vehicle via aerodynamic drag reduction," *Transp Res D Transp Environ*, vol. 15, no. 5, pp. 275–284, 2010, doi: https://doi.org/10.1016/j.trd.2010.02.010.

[4] B., . H., E. A. Kosasih, R. F. Karim, and J. Julian, "Drag reduction by combination of flow control using inlet disturbance body and plasma actuator on cylinder model," *Journal of Mechanical Engineering and Sciences*, vol. 13, no. 1, pp. 4503–4511, Mar. 2019, doi: 10.15282/jmes.13.1.2019.12.0382.

[5] W. Tomasz, K. Jaroslaw, and M. Magda, "Influence of the use of electric drive in a glider on its aerodynamic parameters on the example of GP-15 glider," in *NTinAD 2020 - New Trends in Aviation Development 2020 - 15th International Scientific Conference, Proceedings*, Sep. 2020, pp. 254–258. doi: 10.1109/NTAD51447.2020.9379086.

[6] J. P. R. Suárez, D. V. Castillo, and E. F. Solano, "Experimental and CFD Study of a Centrifugal Fan Performance Under ANSI/AMCA Standard," *International Journal on Engineering Applications (IREA)*, vol. 9, no. 6, 2021, [Online]. Available: https://www.praiseworthyprize.org/jsm/index.php?journal=irea&page=article&op=view&path%5B%5D=25247

[7] J. Julian, Harinaldi, Budiarso, C.-C. Wang, and M.-J. Chern, "Effect of plasma actuator in boundary layer on flat plate model with turbulent promoter," *Proc Inst Mech Eng G J Aerosp Eng*, vol. 232, no. 16, pp. 3001–3010, 2018, doi: 10.1177/0954410017727301.

[8] N. Beck, T. Landa, A. Seitz, L. Boermans, Y. Liu, and R. Radespiel, "Drag Reduction by Laminar Flow Control," *Energies (Basel)*, vol. 11, no. 1, 2018, doi: 10.3390/en11010252.

[9] Harinaldi, Budiarso, J. Julian, and M. N. Rabbani, "The effect of plasma actuator on the depreciation of the aerodynamic drag on box model," in *AIP Conference Proceedings*, Jun. 2016, vol. 1737. doi: 10.1063/1.4949292.

[10] K. Arabacı and S. Pakdemirli, "Aerodynamically Efficient Bus Designs Inspired by Beluga Whales," 2015. [Online]. Available: https://www.researchgate.net/publication/333310693

[11] H. Chowdhury, R. Islam, M. Hussein, M. Zaid, B. Loganathan, and F. Alam, "Design of an energy efficient car by biomimicry of a boxfish," in *Energy Procedia*, 2019, vol. 160, pp. 40–44. doi: 10.1016/j.egypro.2019.02.116.

[12] A. Altaf, A. A. Omar, and W. Asrar, "Passive drag reduction of square back road vehicles," *Journal of Wind Engineering and Industrial Aerodynamics*, vol. 134, pp. 30–43, 2014, doi: 10.1016/j.jweia.2014.08.006.

[13] S. Peng, X. Liu, Z. Li, and F. Jiang, "Application of Bionics of Tiger Beetle to Aerodynamic Optimization of MIRA Fastback Model," *DEStech Transactions on Computer Science and Engineering*, 2018.

[14] S. Sudhakar and N. Karthikeyan, "Flow Separation Control on a NACA-4415 Airfoil at Low Reynolds Number," in *Lecture Notes in Mechanical Engineering*, 2021, pp. 323–334. doi: 10.1007/978-981-15-5183-3_35.

[15] I. H. Abbott and A. E. von Doenhoff, "THEORY OF WING SECTIONS Including a Summary of Airfoil Data."

[16] J. Julian, W. Iskandar, and F. Wahyuni, "Effect of Single Slat and Double Slat on Aerodynamic Performance of NACA 4415," 2022.

[17] F. Deng, C. Xue, and N. Qin, "Parameterizing Airfoil Shape Using Aerodynamic Performance Parameters," *AIAA Journal*, vol. 0, no. 0, pp. 1–14, doi: 10.2514/1.J061464.

[18] M. A. Raj Mohamed, U. Guven, and R. Yadav, "Flow separation control of NACA-2412 airfoil with bio-inspired nose," *Aircraft Engineering and Aerospace Technology*, vol. 91, no. 7, pp. 1058–1066, Aug. 2019, doi: 10.1108/AEAT-06-2018-0175.

[19] E. Espinel, J. Rojas, and E. F. Solano, "Computational Fluid Dynamics Study of NACA 0012 Airfoil Performance with OpenFOAM®," *International Review of Aerospace Engineering (IREASE)*, vol. 14, no. 4, 2021, [Online]. Available: https://praiseworthyprize.org/jsm/index.php?journal=irease&page=article&op=view&path%5B%5D=24909

[20] J. Julian, W. Iskandar, F. Wahyuni, and F. Ferdyanto, "COMPUTATIONAL FLUID DYNAMICS ANALYSIS BASED ON THE FLUID FLOW SEPARATION POINT ON THE UPPER SIDE OF THE NACA 0015 AIRFOIL WITH THE COEFFICIENT OF FRICTION," *Media Mesin: Majalah Teknik Mesin*, vol. 23, no. 2, pp. 70–82, 2022.

[21] Harinaldi, A. S. Wibowo, J. Julian, and Budiarso, "The comparison of an analytical, experimental, and simulation approach for the average induced velocity of a dielectric barrier discharge (DBD)," *AIP Conf Proc*, vol. 2062, no. 1, p. 20027, 2019, doi: 10.1063/1.5086574.

[22] A. Seeni and P. Rajendran, "Numerical Validation of NACA 0009 Airfoil in Ultra-Low Reynolds Number Flows," *International Review of Aerospace Engineering (IREASE)*, vol. 12, no. 2, 2019, [Online]. Available: https://www.praiseworthyprize.org/jsm/index.php?journal=irease&page=article&op=view&path%5B%5D=22925

[23] W. Iskandar, J. Julian, F. Wahyuni, F. Ferdyanto, H. K. Prabu, and F. Yulia, "Study of Airfoil Characteristics on NACA 4415 with Reynolds Number Variations," *International Review on Modelling and Simulations (IREMOS)*, vol. 15, no. 3, pp. 162–171, Jun. 2022.

[24] S. M. A. Aftab, A. S. M. Rafie, N. A. Razak, and K. A. Ahmad, "Turbulence model selection for low reynolds number flows," *PLoS One*, vol. 11, no. 4, Apr. 2016, doi: 10.1371/journal.pone.0153755.

[25] F. Marchetto and E. Benini, "Numerical Simulation of Harmonic Pitching Supercritical Airfoils Equipped with Movable Gurney Flaps," *International Review of Aerospace Engineering (IREASE)*, vol. 12, no. 3, 2019, [Online]. Available: https://www.praiseworthyprize.org/jsm/index.php?journal=irease&page=article&op=view&path%5B%5D=23336

[26] J. Julian, W. Iskandar, F. Wahyuni, and N. T. Bunga, "Characterization of the Co-Flow Jet Effect as One of the Flow Control Devices," *Jurnal Asiimetrik: Jurnal Ilmiah Rekayasa & Inovasi*, pp. 185–192, 2022.

[27] J. Julian, W. Iskandar, F. Wahyuni, and dan Nely Toding Bunga, "Aerodynamic Performance Improvement on NACA 4415 Airfoil by Using Cavity," vol. 5, pp. 135–142, 2023.

[28] J. Julian, W. Iskandar, and F. Wahyuni, "Aerodynamics Improvement of NACA 0015 by Using Co-Flow Jet," *International Journal of Marine Engineering Innovation and Research*, vol. 7, no. 4, Dec. 2022, doi: 10.12962/j25481479.v7i4.14898.

[29] P. J. Boache, "Perspective: A Method for Uniform Reporting of Grid Refinement Studies," 1994. [Online]. Available: http://fluidsengineering.asmedigitalcollection.asme.org/

[30] P. Kekina and C. Suvanjumrat, "A Comparative Study on Turbulence Models for Simulation of Flow Past NACA 0015 Airfoil Using OpenFOAM."

[31] E. N. Jacobs and A. Sherman, "Airfoil section characteristics as affected by variations of the Reynolds number," *NACA Technical Report*, vol. 586, pp. 227–267, 1937.

[32] C.-S. Lee, W. Pang, S. Srigrarom, D.-B. Wang, and F.-B. Hsiao, "CLASSIFICATION OF AIRFOILS BY ABNORMAL BEHAVIOR OF LIFT CURVES AT LOW REYNOLDS NUMBER," in *24th AIAA Applied Aerodynamics Conference*, doi: 10.2514/6.2006-3179.

[33] H. Bao, W. Yang, D. Ma, W. Song, and B. Song, "Numerical simulation of flapping airfoil with alula," *International Journal of Micro Air Vehicles*, vol. 12, 2020, doi: 10.1177/1756829320977989.

[34] H. Harinaldi, B. Budiarso, F. Megawanto, R. Karim, N. Bunga, and J. Julian, "Flow Separation Delay on NACA 4415 Airfoil Using Plasma Actuator Effect," *International Review of Aerospace Engineering (IREASE)*, vol. 12, no. 4, 2019, [Online]. Available: https://www.praiseworthyprize.org/jsm/index.php?journal=irease&page=article&op=view&path%5B%5D=23054

[35] J. Julian, H. Harinaldi, B. Budiarso, R. Difitro, and P. Stefan, "The Effect of Plasma Actuator Placement on Drag Coefficient Reduction of Ahmed Body as an Aerodynamic Model," *International Journal of Technology*, vol. 7, no. 2, 2016, [Online]. Available: http://ijtech.eng.ui.ac.id/old/index.php/journal/article/view/2994

[36] F. C. Megawanto, Harinaldi, Budiarso, and J. Julian, "Numerical analysis of plasma actuator for drag reduction and lift enhancement on NACA 4415 airfoil," *AIP Conf Proc*, vol. 2001, no. 1, p. 50001, 2018, doi: 10.1063/1.5049992.

[37] J. Julian, R. F. Karim, Budiarso, and Harinaldi, "Review: Flow control on a squareback model," *International Review of Aerospace Engineering*, vol. 10, no. 4, pp. 230–239, 2017, doi: 10.15866/irease.v10i4.12636.

[38] Budiarso, Harinaldi, Karim Riza Farrash, and Julian James, "Drag reduction due to recirculating bubble control using plasma actuator on a squareback model," *MATEC Web Conf.*, vol. 154, p. 1108, 2018, doi: 10.1051/matecconf/201815401108.

[39] A. Choudhry, M. Arjomandi, and R. Kelso, "A study of long separation bubble on thick airfoils and its consequent effects," *Int J Heat Fluid Flow*, vol. 52, pp. 84–96, Apr. 2015, doi: 10.1016/j.ijheatfluidflow.2014.12.001.

[40] V. A. Frolov, "Laminar separation point of flow on surface of symmetrical airfoil," in *AIP Conference Proceedings*, Oct. 2016, vol. 1770. doi: 10.1063/1.4963995.